

PHYSICAL REVIEW LETTERS

VOLUME 45

29 DECEMBER 1980

NUMBER 26

Test of Relativistic Gravitation with a Space-Borne Hydrogen Maser

R. F. C. Vessot, M. W. Levine,^(a) E. M. Mattison, E. L. Blomberg, T. E. Hoffman,^(b)
G. U. Nystrom, and B. F. Farrel

Smithsonian Astrophysical Observatory, Cambridge, Massachusetts 02138

and

R. Decher, P. B. Eby, C. R. Baugher, J. W. Watts, D. L. Teuber, and F. D. Wills
George C. Marshall Space Flight Center, Huntsville, Alabama 35812

(Received 19 August 1980)

The results of a test of general relativity with use of a hydrogen-maser frequency standard in a spacecraft launched nearly vertically upward to 10 000 km are reported. The agreement of the observed relativistic frequency shift with prediction is at the 70×10^{-6} level.

PACS numbers: 04.80.+z

A test of relativistic gravitation involving frequency comparison by continuous wave microwave signals generated from hydrogen masers located in a spacecraft and at an Earth station was performed jointly by the National Aeronautics and Space Administration and by the Smithsonian Astrophysical Observatory. The 100-kg spin-stabilized spacecraft was launched by a Scout Rocket to an altitude of 10 000 km in a nearly vertical trajectory. The results of this experiment extend our confidence in predictions made according to the general theory of relativity to the 70×10^{-6} level.

The measuring scheme, shown in Fig. 1, provided one-way and two-way Doppler information by simultaneous transmission of three microwave signals. The first-order Doppler shifts ($\Delta f/f \sim 10^{-5}$) in the space clock signal were removed by subtracting in mixer M3 one-half the two-way Doppler shift obtained from mixer M2 by comparing the separate two-way transponder links. The trajectory of the space probe was computed from two-way Doppler data obtained at the main tracking station at Merrit Island, Florida,

and three-way Doppler data obtained at additional stations at Bermuda, Greenbelt, Maryland, and Ascension Island.

Since all three microwave links operated simultaneously, frequency separation, required to prevent regeneration, was obtained by using ration-

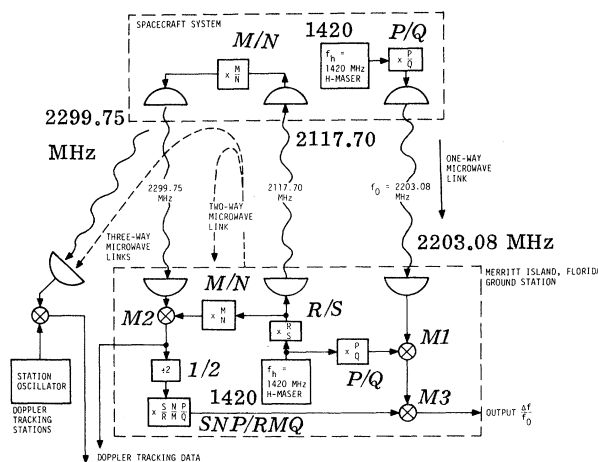


FIG. 1. Doppler cancellation and tracking system.

al multiples of the maser output frequency, $f_H = 1420.405\,751$ MHz. The standard U.S.B. 240/221 ratio shown as M/N in Fig. 1 was used in the transponder. The separation of frequencies causes an appreciable $1/f^2$ dispersion effect from the time-varying ionospheric columnar electron density during the mission. The ionospheric Doppler contribution from the f^{-2} component was eliminated by choosing the Earth-station uplink frequency $f_H R/S$ and probe-maser downlink frequency $f_H P/Q$ according to the relationship¹ $P/Q - \sqrt{2}(R/S)[1 + (N/M)^2]^{-1/2} = 0$.

With $P/Q = \frac{76}{49}$ and $R/S = \frac{82}{55}$, the equation is satisfied to within 2×10^{-5} , which for the worst-case ionospheric conditions possible during the end of the flight would produce an error of 2×10^{-15} in $\Delta f/f$.

According to the general theory of relativity, the Doppler-canceled frequency from mixer M3, when normalized to the maser downlink frequency f_0 , is given by²

$$\frac{\Delta f}{f_0} = \frac{\varphi_s - \varphi_e}{c^2} - \frac{|\vec{v}_e - \vec{v}_s|^2}{2c^2} - \frac{\vec{r}_{se} \cdot \vec{a}_e}{c^2}. \quad (1)$$

For this expression we have adopted an Earth-centered inertial coordinate frame. The Newtonian gravitational potentials φ_s and φ_e are for the spacecraft and Earth, respectively, and the first term of Eq. (1) is identified with the gravitational red shift. The second term, involving the relative velocity $|\vec{v}_e - \vec{v}_s|$ between Earth and spacecraft, is identified with the second-order Doppler effect of special relativity. The third term describes the residual first-order Doppler shift due to acceleration, \vec{a}_e , of the Earth station during the light time $|\vec{r}_{se}/c|$. Here \vec{r}_{se} is the vector from spacecraft to Earth. The Doppler and ionospheric cancellations are effective for frequency measurements made over time average τ greater than r_{se}/c (i.e., $\tau > 0.03$ sec).

The goal of the experiment was to compare the frequency variations predicted by Eq. (1) with the observed data at a level of precision consistent with the maser stability, which, for 100 sec averaging time,³ is approximately 1 part in 10^{14} .

Because of the up-down trajectory, little time was available after launch for thermal restabilization and accommodation to 0-g from the 18-g thrust of the four-stage rocket motor. The overall system was designed so that phase and frequency perturbations resulting from launch should have settled down well before the spacecraft reached apogee.

The output from mixer M3 is the beat signal Δf ,

described by Eq. (1), encoded with 14-bit accuracy every 0.01 sec and referenced in time to the tracking network clocks for correlation with trajectory data. Samples of analog strip-chart recordings of Δf are shown in Fig. 2 (2 div = 1 sec). The experiment started at 11:46 GMT (Greenwich mean time) after separation of the last rocket stage. The probe slows down while ascending, which results in a decreasing second-order Doppler shift and beat frequency. At 11:49 GMT red shift and second-order Doppler shift are equal and opposite as indicated by a zero beat and phase reversal. At apogee, 12:40 GMT, the red shift is approximately 0.9 Hz. During descent zero beat occurs again at 13:31 GMT and the beat fre-

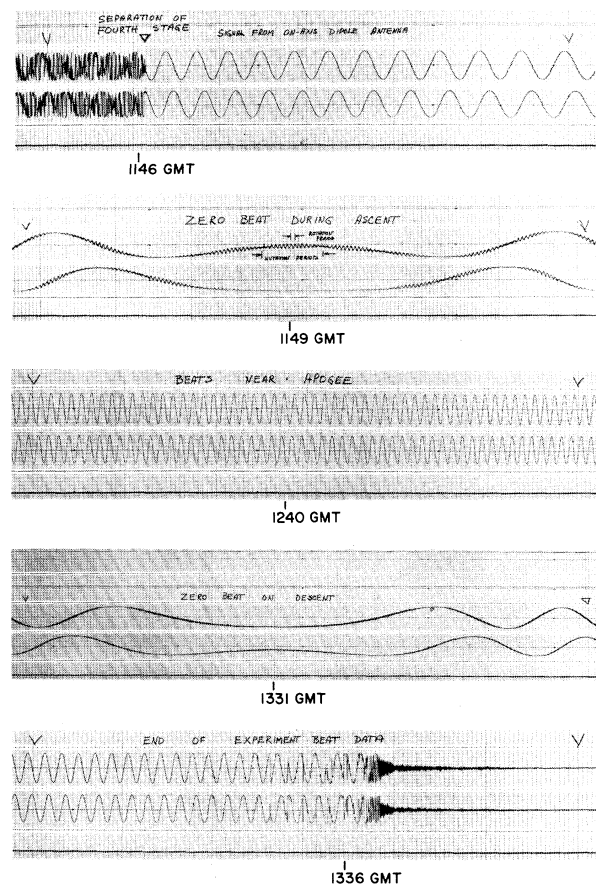


FIG. 2. Analog strip-chart recorder data at various times during the mission. (a) Signal from dipole antenna. The (inverted delta) markers indicate the time at which the fourth stage of the rocket separated. (b) Zero beat during ascent. The small interval indicated above the top trace is a rotation period; the longer interval below is a nutation period. (c) Beats near apogee. (d) Zero beat on descent. (e) End of experimental beat data.

quency increases until impact into the Atlantic Ocean at 13:36 GMT. Near the end of the flight, at 13:36 GMT, the uplink transmission was interrupted for 2 min (because of a ground-transmitter problem), which introduced a phase transient whose behavior cannot be accounted for. Therefore, data beyond this time were not used in the present conclusions.

Comparison of observed frequency variations with the prediction, obtained from trajectory and geopotential data in Eq. (1), was done in terms of phase. The average slope of observed minus predicted phase was -2.9×10^{-13} in $\Delta f/f$ for a 500-sec interval centered at apogee. For convenience of computation this slope (caused by a fixed frequency offset between the two clocks) was removed to obtain zero frequency residual at apogee. Corrections listed in Table I were applied to remove errors from known sources. These corrections were derived from careful calibration of the payload before flight in a series of thermal vacuum tests under simulated flight conditions including the effects of magnetic fields varying in magnitude and direction, vehicle spin variations, barometric pressure, and temperature. Variations of these parameters during flight were measured by telemetry and applied in the corrections.

Figure 3 presents the frequency variation $\Delta f/f_0$ predicted from Eq. (1) together with the final residual $\Delta f/f$ after corrections and smoothing with a 100-sec Hanning filter. The residual frequency was sampled at 100-sec intervals. The linear regression of these data points on the prediction from Eq. (1) gives the following fit to the data:

$$\frac{\Delta f}{f} \Big|_R = [1 + (2.5 \pm 63) \times 10^{-6}] \times \left(\frac{\varphi_s - \varphi_e}{c^2} - \frac{|\vec{v}_s - \vec{v}_e|}{2c^2} - \frac{\vec{r}_{se} \cdot \vec{a}_e}{c^2} \right).$$

Errors from apparatus bias and trajectory uncertainty, shown in Table I, may contribute possible bias uncertainty of 31.8×10^{-6} in the linear fit. Combining the statistical uncertainty of the slope with the possible bias as root sum squares we have, for the overall uncertainty in the test,

$$\frac{\Delta f}{f} = [1 + (2.5 \pm 70) \times 10^{-6}] \times \left(\frac{\varphi_s - \varphi_e}{c^2} - \frac{|\vec{v}_s - \vec{v}_e|}{2c^2} - \frac{\vec{r}_{se} \cdot \vec{a}_e}{c^2} \right).$$

Previous tests by Pound and co-workers⁴ con-

TABLE I. Sources of possible bias errors.

Parameter	Correction formula	Range of variable		1-standard-deviation contribution of uncertainty to $\Delta f/f$
		12:15-12:40 GMT	12:40-13:22 GMT	
Axial magnetic field from trajectory	$f^{-1}\Delta f/\Delta H = (-5.8992 \pm 0.567) \times 10^{-13}/\text{Oe to apogee}$ $f^{-1}\Delta f/\Delta H = (-12.7213 \pm 0.894) \times 10^{-13}/\text{Oe from apogee}$	-0.98×10^{-2} Oe	$+3.36 \times 10^{-2}$ Oe	$\pm 0.6 \times 10^{-15}$ $\pm 3.0 \times 10^{-15}$
Maser oven temperature (voltage)	$f^{-1}\Delta f/\Delta V = (-3.60 \pm 0.60) \times 10^{-14}/\text{V}$	-0.25 V	$+0.25$ V	$\pm 1.5 \times 10^{-15}$
Maser outer can pressure	$f^{-1}\Delta f/\Delta P = (-310.8 \pm 4.3) \times 10^{-14}/\text{psi}$ $f^{-1}\Delta f/\Delta \Omega = [-(1.435 \pm 0.48) + (0.148 \pm 0.0084)\Omega] \times 10^{-15}/\text{rpm}$	$+0.02$ psi	$+0.02$ psi	$\pm 1.7 \times 10^{-15}$
Probe rotation rate	Trajectory uncertainties expressed in terms of $\Delta v^2/2c^2$ and $\Delta \phi^2/c^2$ Root-sum-square estimate of overall possible bias	$+1.4$ rpm	$+1.8$ rpm	$\pm 4.6 \times 10^{-15}$ $\pm 3.3 \times 10^{-15}$ $\pm 6.8 \times 10^{-15}$

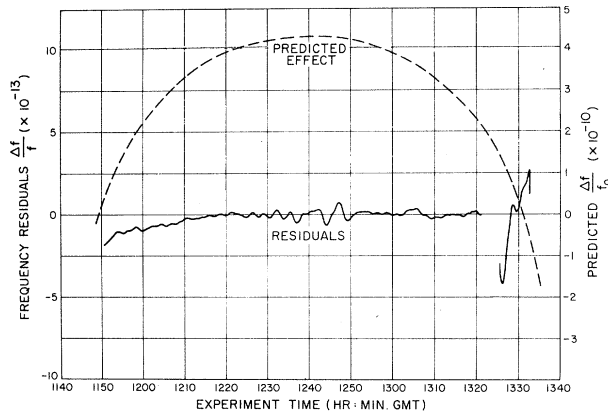


FIG. 3. Frequency residuals and predicted effect during mission.

firm the predicted gravitational shift of spectral lines of γ radiation of ^{57}Fe at the 10^{-2} level. Confirmation of the time dilation at the 10^{-3} level has been reported by Bailey *et al.*⁵ from muon-decay experiments. A test of the isotropicity of space at the $\Delta l/l \approx 10^{-15}$ level, by measuring the length of a laser resonator oriented in various directions, has been done by Brilliet and Hall.⁶ Since the experiment measured the combined effects of relativistic gravity and special relativity in Eq. (1), we do not believe it is appropriate to account for these separately in view of the fact that the comparison was made across regions of space-time having considerable curvature and

that previous tests were essentially "local" in nature. We conclude from our results that the relativistic and gravitational factors affecting the frequency of the observed signals and governing the velocity of light are consistent with theory at the 70×10^{-6} level of accuracy.

We wish to express our profound appreciation for support and assistance from the National Aeronautics and Space Administration and particularly for the encouragement of Dr. N. G. Roman. We gratefully thank the highly competent technical and administrative staffs of the NASA Marshall Space Flight Center and the Smithsonian Astrophysical Observatory, who cooperated very closely throughout this program.

(a) Present address: Frequency and Time Systems, 34 Tozer Rd., Beverly, Mass. 01915.

(b) Present address: Arthur D. Little Inc., 25 Acorn Park, Cambridge, Mass. 02140.

¹R. F. C. Vessot and M. W. Levine, in *Proceedings of the Twenty-Eighth Annual Symposium on Frequency Control* (U.S. Army Electronics Command, Ft. Monmouth, N. J., 1974), pp. 408–414.

²D. Kleppner, R. F. C. Vessot, and N. F. Ramsey, *Astrophys. Space Sci.* **6**, 13–32 (1970).

³D. W. Allan, *Proc. IEEE* **54**, 221–230 (1966).

⁴R. V. Pound and S. A. Rebka, *Phys. Rev. Lett.* **4**, 337–341 (1960); R. V. Pound and J. L. Snider, *Phys. Rev.* **140**, B788–B803 (1965).

⁵J. Bailey *et al.*, *Nature (London)* **218**, 301–302 (1977).

⁶A. Brilliet and J. L. Hall, *Phys. Rev. Lett.* **42**, 549–552 (1979).

CP Nonconservation in Three-Neutrino Oscillations

V. Barger and K. Whisnant

Physics Department, University of Wisconsin-Madison, Madison, Wisconsin 53706

and

R. J. N. Phillips

Rutherford Laboratory, Chilton, Didcot, Oxon OX11 0QX, England

(Received 10 November 1980)

Direct *CP* tests in neutrino oscillations require comparison of off-diagonal channels $\nu_\alpha \rightarrow \nu_\beta$ with *CP*-conjugate channels $\bar{\nu}_\alpha \rightarrow \bar{\nu}_\beta$ (or with $\nu_\beta \rightarrow \nu_\alpha$ by assuming *CPT* invariance). For the three-neutrino case, it is shown that *CP*-nonconservation effects are identical in all three available channels $\nu_e \leftrightarrow \nu_\mu$, $\nu_\mu \leftrightarrow \nu_\tau$, and $\nu_\tau \leftrightarrow \nu_e$, and argued that they could be large and measurable in meson factory experiments. Indirect *CP* tests include the correlation of average probabilities.

PACS numbers: 14.60.Gh, 11.30.Er, 13.15.+g

Possible *CP* nonconservation in neutrino oscillations is interesting because it relates directly to *CP*-nonconserving (*CPN*) phase parameters in

the mixing matrix for $n \geq 3$ nondegenerate neutrinos.¹ However, there are already stringent experimental limits on neutrino oscillations in

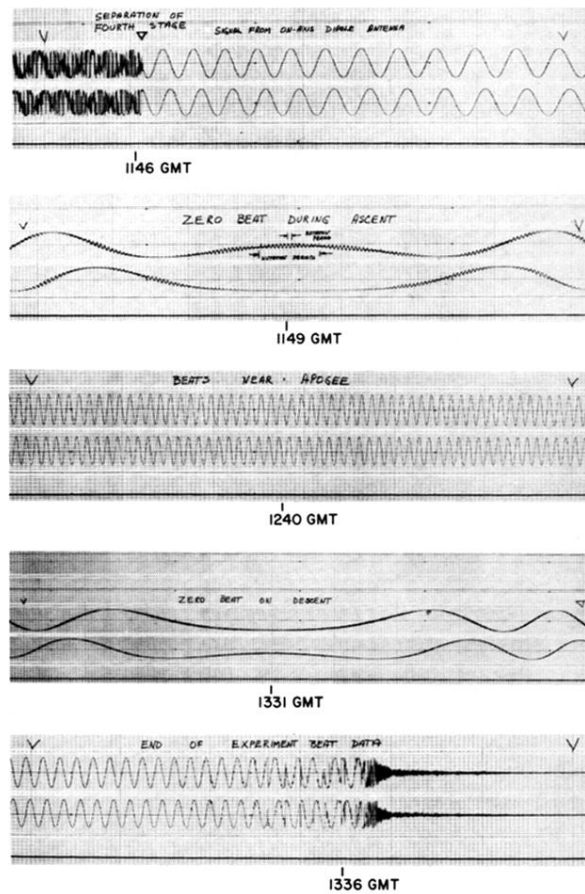


FIG. 2. Analog strip-chart recorder data at various times during the mission. (a) Signal from dipole antenna. The (inverted delta) markers indicate the time at which the fourth stage of the rocket separated. (b) Zero beat during ascent. The small interval indicated above the top trace is a rotation period; the longer interval below is a nutation period. (c) Beats near apogee. (d) Zero beat on descent. (e) End of experimental beat data.